Development of a Direct Analysis Method for Copper in Serum by Tungsten Filament Electrothermal Atomic Absorption

by Reema Shakya, Bachelor of Science

A Thesis Submitted in Partial
Fulfillment of the Requirements
for the Degree of
Master of Science
in the field of Chemistry

Advisory Committee

Edward C. Navarre

Eric J. Voss

Myron W. Jones

Graduate School
Southern Illinois University Edwardsville
December, 2014

ProQuest LLC.
789 East Eisenhower Parkway
P.O. Box 1346
Ann Arbor, MI 48106 - 1346

ABSTRACT

DEVELOPMENT OF A DIRECT ANALYSIS METHOD FOR COPPER IN SERUM BY TUNGSTEN FILAMENT ELECTROTHERMAL ATOMIC ABSORPTION

by

REEMA SHAKYA

Advisor: Professor Edward C. Navarre

The analysis of horse serum samples for copper is relevant to biomarkers for a variety of pathologies in humans. The inexpensive and compact nature of locally laboratory built tungsten filament electrothermal atomic absorption spectrometry instruments (WETAAS) makes them well suited to copper analysis in the clinical context; however, little research in this area exists. This project was undertaken to determine the experimental conditions necessary for determining copper in serum by WETAAS without resorting to sample digestion. Serum samples were prepared by 1:5 dilution in 0.2% nitric acid solution. The filament positioning with the light path plays an important role in the actual number of vaporized atoms of analyte being detected. In aqueous calibration standards, ammonium dihydrogen phosphate was found to be a critical matrix modifier, but in the presence of serum as an interference, the matrix modifier was not of much use. The results indicate that the serum matrix strongly suppresses the copper analytical signal. The merits of using integrated area for quantitation rather than peak height was found in the complex matrix system. Then the background concentration of copper in serum was determined by the standard additions method. Then the same samples were analyzed using a standard method for analysis of copper in serum through flame atomic absorption spectrometry, which is a matrix interference independent system.

ACKNOWLEDGMENTS

I am grateful to Dr. Edward Navarre for giving me an opportunity to work under his supervision. I would like to thank my parents and my husband for their immense support, which made me able to reach here. I am thankful to my lab mates and friends for their help. I would like to thank the SIUe Graduate School and the SIUe Department of Chemistry for providing me with the assistantship. I would also like to thank The Sigma Aldrich Corporation and The Goldberg Science Foundation for funding our project.

TABLE OF CONTENTS

LIST OF FIGURES

LIST OF TABLES

CHAPTER I

INTRODUCTION

1.1. Copper (Cu)

Copper is the 25th most abundant element in the earth's crust. It is a reddish colored semi noble metal, occasionally in native form and mostly occurs in the form of copper minerals in soil, water, sediments and rocks. It has excellent heat conductivity so it is frequently used in the electrical industry. It is an essential trace element as a constituent of copper proteins with enzyme activity for humans, higher mammals, and plants. Similarly, it stores calcium in bones and also repairs or builds connective tissues. It can be ingested through seeds, grains, nuts, meat, eggs, chocolate, and contaminated water, while it can be inhaled during plumbing and welding. [1,2] Copper is one of the contaminants of drinking water, so the Environmental Protection Agency (EPA) has determined the maximum contaminant level (MCL) of copper in drinking water as 1.3 mg/L.[3]

Copper acts as a neurotransmitter in the Central Nervous System (CNS) so, improper concentration of it leads to behavioral disorders, fatigue, and depression. A normal adult human should contain 11-22 μmol/L of copper, which gives 50- 80 mg in total mass in the body. A normal horse should contain about 13 μmol/L of copper in serum *i.e.* about 730 ng/mL which is similar to that of a human.[4,5] The copper concentration in the body increases when there are deficiencies of iron, manganese, zinc, vitamin B, and vitamin C. Therefore, it acts as a sensitive biomarker for human pathologies. In the case of the copper and zinc proportion in the body, the ratio should be 0.7 to 1.0. If there is an increase in this ratio, it indicates harmful inflammation (Erythrocytes Sedimentation Rate and Interlukin-6) or nutritional changes (albumin, Body Mass Index). The excess copper gets accumulated in the liver and then gets transported to different organs and soft tissues of the body. The example

of chronic intoxication of copper deposition in the soft tissues like the eye leads to the formation of a ring of it in the cornea, known as Wilson's disease, which is mostly hereditary. Acute and chronic copper intoxication can be treated with chelator therapy by using D-penicillamine and meso-2,3-dimercaptosuccinic acid (DMSA). These chelating agents bind with the free copper in blood and excrete it in urine.[6,7]

1.2. Atomic Absorption Spectroscopy (AAS)

If energy of the right wavelength gets absorbed by the atom, then it can lead the outer shell electron to reach the excited state, which is unstable. This excited electron is capable of returning to the ground state by emitting the energy it absorbed. The wavelength of the emitted light energy depends on the electronic transition of each element.[8]

Atomic absorption can be defined as the amount of light of a required wavelength that is absorbed by the atomic cloud. The atomic cloud is produced by supplying the thermal energy that dissociates the molecular chemical compounds into free atoms. Quantitative determination of the absorption depends on the initial intensity (I_o) and the reduced intensity (I) measured by the detector. [8]

$$A = \log (I_0/I) \quad (1)$$

This is the mathematical representation of absorbance (A). The absorbance of the light increases as the number of atoms in the light path increases, resulting in a decrease in the initial intensity of light. The relation between absorbance of light and concentration of sample can be given by Beer's Law. [8]

$$A = abc \quad (2)$$

Where, *a* is absorptivity, *b* is path length and *c* is concentration of the sample.

Atomic spectroscopy consists of a primary light source - a hollow cathode lamp (HCL) and a sample cell and a detector arranged in a sequence. The primary light source

produces the specific wavelength of light given off to the atomized sample. The sample cell is either a flame or a non-flame, which is used to atomize analytes that can be measured by the detector. The most common non-flame sample cell is the electrothermal atomizer.

1.2.1. Electro Thermal Atomic Absorption Spectrometry (ETAAS)

Electrothermal atomization is accomplished by the passage of electrical current through the sample cell. The atomizer is heated through series of programmable steps for specific lengths of time, which depends on the atomizer itself.[6] The ideal atomizer should be chemically inert, physically stable, and with a high melting point and a rapid heating rate.[9] The two types of atomizers commonly used are the graphite furnace and the tungsten filament.

There are five steps in the ETAAS process. The first step is drying, in which the sample is heated at a low temperature to dry it to the solid form by evaporating the solvent, such as water and acid present in it. This step is performed at a low temperature for a long period of time to avoid sample spattering for better precision. Second, the pyrolysis is the step that is also known as the ashing, charring, and pretreatment step. In this step the volatilization of the organic and inorganic matrix component takes place selectively using a higher temperature than drying to remove the interferences from atomization. The temperature of this step should be below the temperature at which any loss of the analyte occurs. Pyrolysis is followed by a pause or cool down; in this step the filament is cooled down to maximize the heating rate and extend the isothermal zone during atomization and improve the sensitivity of the process. This step also allows time for the matrix vapors to escape from the enclosure, which decreases the matrix interference. During the atomization step the temperature is increased to vaporize and dissociate the volatilized molecular species producing an atomic vapor of the analyte elements from which the atomic absorption is

measured. The temperature selected depends on the analyte as at very high temperature ionization can occur. Finally, the cleaning step is performed at a higher temperature than other steps to remove any of the sample residue and make the atomizer ready for the next heating cycle.[8]

The best conditions for pyrolysis and atomization are extracted from the graph of integrated area or peak height of the atomic absorption signal versus temperature. An example of this type of plot is shown in Fig.1. In the pyrolysis step, there should not be any loss of analyte, so the experimentally detected decrease in the analytical signal is taken as the limiting pyrolysis temperature. In the atomization step, the optimum atomization temperature is chosen at the lowest temperature that causes complete atomization with the least amount of error. In the figure below the curve on the left corresponds to pyrolysis and one on the right to atomization. [8]

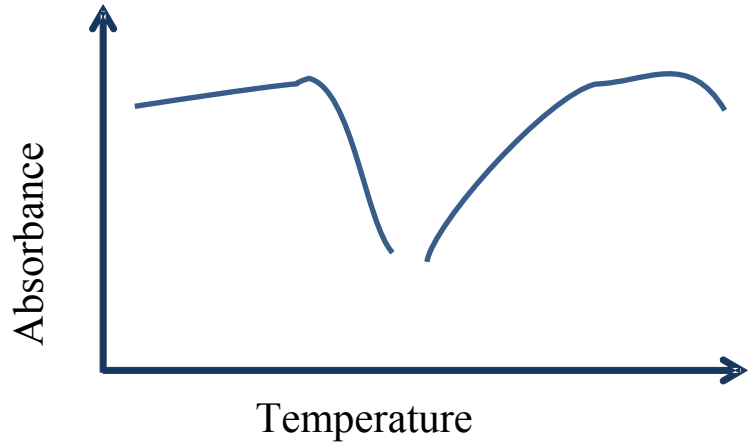

Figure 1. The Pyrolysis and Atomization Curve

1.2.1.1. Graphite Furnace ETAAS. The graphite furnace atomization technique is advanced and widely used for ETAAS. Graphite tubes are used as the atomizer, through which the light path passes. A few microliters of sample solution are quantitatively placed into the graphite tube, through a sample injection hole located in the center of the tube wall. The tube is heated

through the programmed heating cycle of different steps until finally the analyte present in the sample is dissociated into atoms and atomic absorbance occurs. During the atom formation and diffusion out of the furnace, the absorbance signal is measured, and analyzed for peak height and integrated area for quantitation.[6] The graphite furnace has a limit of detection of 0.005-0.4 µg/L, accuracy < 10 % relative error, and precision of ± 2-5 % relative standard deviation.[10,11]

During the heating process of the graphite tubes there is an uneven temperature in the ends of the tube. Therefore, a platform is introduced in the graphite tube. The platform is heated by radiation so there is a uniform temperature with fewer interferences. Graphite furnace instruments are complex and bulky and need a 2 KW power supply. There are difficulties in the determination of elements that form refractory carbides because the atomizer is made of carbon.[12] Due to these reasons there is a demand for an analytical instrument for lower detection limit and reasonable cost.

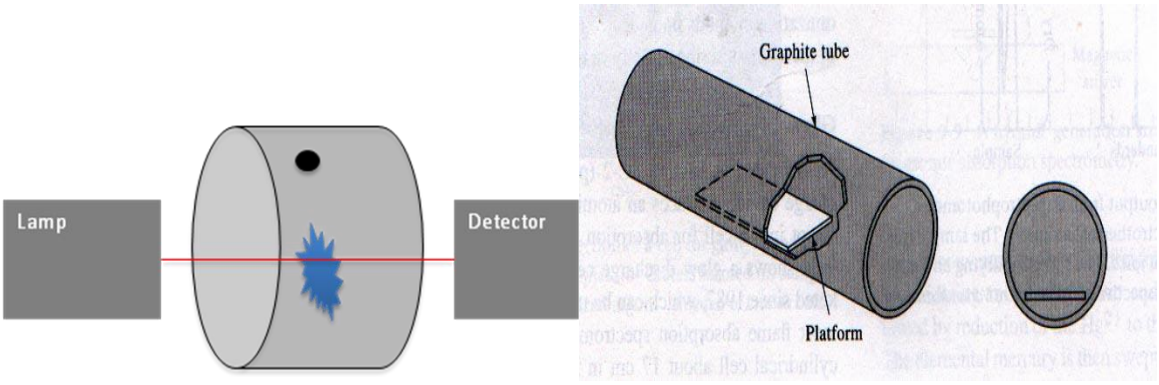

Figure 2. Graphite Furnace AAS Instrumentation and the Graphite Tube.[13]

1.2.1.2. Tungsten ETAAS. Tungsten coil atomic spectrometric instruments are miniaturized and portable instrumentation for elemental analysis.[14] Tungsten coil atomizers were first proposed in 1972 by Williams and Piepmeier[15], in which a tungsten filament extracted from a 24 W commercial Osram halogen projector bulb was used for copper and calcium analysis.

In 1988, Berndt and Schaldach used a tungsten coil from a commercial 12 V, 150 W projector light bulb to determine 13 elements in synthetic urine samples.[16]

Tungsten is a perfect material for resistively heated atomizers as it has high melting point (3680 K), low vapor pressure (1.59×10^{-6} Pa at 2400 K) and a very low specific heat of 0.132 $Jg^{-1}K^{-1}$.[13] The low specific heat results in, a high heating rate of 30 Kms^{-1} compared to 2-4 Kms^{-1} for GFAAS.[9,15]Therefore, a simple, low-voltage power supply can be used to reach high temperatures without melting the atomizer. The Osram bulbs are mass produced, so there is little variation between the coils. Therefore, it gives more reproducible measurements *i.e.* the resistance of filaments has changed only about 7% in 15 years.[13,17] These tungsten coils are inexpensive and are fabricated with high purity tungsten with the lifetime of about 300 heating cycles. The filaments are very stable, inert and have good resistance to harsh chemicals such as hydrochloric, sulfuric and nitric acid. The use of tungsten atomizers makes the instrument fast and portable. In a demonstration of portability, an entire spectrometer was assembled measuring around 50 x 20 x 8 cm and powered by 12V car battery. This type of instrument has low detection limits (ng/L) and high sensitivity but can be used for single element analysis.[9,16]

A tungsten coil has a non-isothermal atmosphere around it. There is relatively lower temperature of gas phase of 600-700 ºC than the atomizer surface, which can lead to formation of molecules like chlorides, oxides and metal dimers. These molecules can produce matrix interference, resulting in a smaller population of analyte atoms. Similarly, analyte-concomittant compounds formed have a negative effect on the sensitivity and accuracy of the instrument. The use of purge gas composed of a low percentage of hydrogen gas dissolved in argon can minimize these two effects. The advantages of tungsten filament atomizers outweighs these drawbacks.[16]

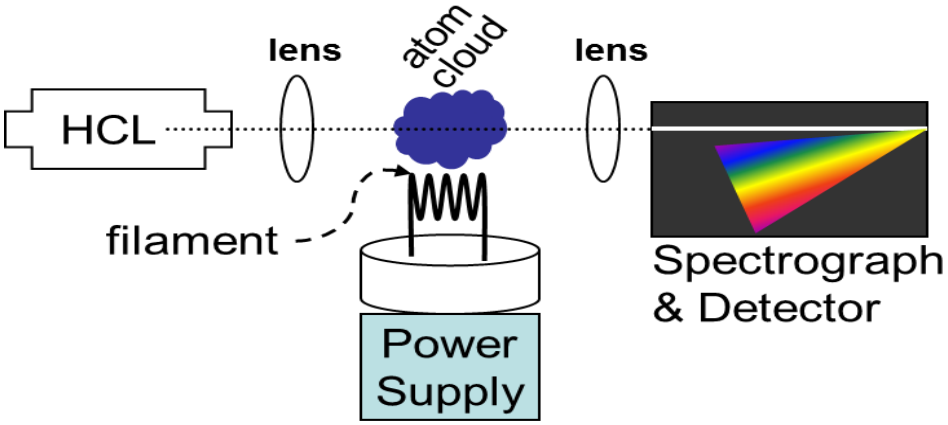

Figure 3. Instrumentation of Tungsten Filament AAS [8]

A representative schematic diagram of a tungsten filament ETAAS instrument is shown in Fig.3. A hollow cathode lamp (HCL) is used as the light source for the excitation of the atoms. Light from the HCL is detected by a charged coupled device (CCD) detector after the analytical wavelength photons are isolated by the spectrograph.

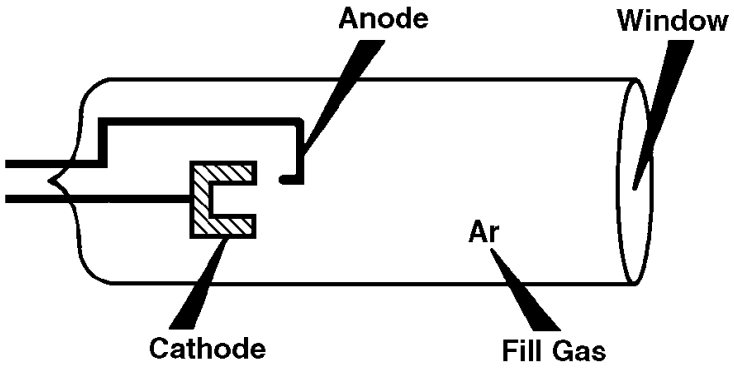

Figure 4. Hollow Cathode Lamp

A hollow cathode lamp consists of a hollowed out cylinder of the metal whose spectrum is to be produced. The metal acts as the cathode and a tungsten rod as the anode. The cathode is sealed in a glass tube filled with argon at a pressure of 1 to 5 torr. As electrical potential is applied between the anode and cathode the argon gas gets ionized. The positively charged argon ions acquire enough kinetic energy to dislodge metal atoms from

the cathode. This process is known as sputtering. As the sputtered atoms are in an excited electronic state, when they return to their ground state these atoms emit radiation of the characteristic wavelengths of those atoms. Each HCL will have a particular current for optimum performance and lamp life. When the HCL begins to deteriorate, the spectral lines begin to shorten and broaden giving reduced sensitivity and accuracy.[8,18]

The standard method for obtaining the concentration of copper in serum is with flame AAS as it has fewer interferences than other instrumentation for elemental analysis. There are several steps for it. The sample is nebulized by a flow of gaseous oxidant, then mixed with a gaseous fuel and carried to a flame for atomization to occur. The dissociation of the analyte into atoms at the atomization step is due to heat energy of the air-acetylene flame, which is 2398 - 2973 K. The design of the premix burner requires a large volume of analyte sample *i.e.*3-8 mL/min, which is a major issue in cases of biological samples.[8]

1.3. Power Supply

Various control modes for the power supply can be used such as current, voltage, power, and radiation. In current-controlled mode the current supplied by the power supply is set to certain values for different heating steps. In voltage-controlled mode the voltage across the atomizer is set to certain values for different heating steps. The power-controlled heating is the product of the voltage and current. In the radiation-controlled heating method, radiation from the filament is used to regulate the electrical power supply. In this mode the radiation transducers, such as phototransistors, can function as a radiation sensing device.[19]

In current-controlled heating, repeated heating of the filament causes it to lose mass and have a smaller cross-sectional area. The thinning effect causes an increase in the resistance of the filament. Similarly, current-controlled heating cannot compensate for the larger resistance, resulting in higher temperatures with successive cycles. Voltage-controlled

heating compensates for the change in resistance, resulting in less temperature drift. Radiation-controlled heating is also able to compensate the change in resistance. In voltage-controlled heating, the increase in resistance allows less current through the atomizer, decreasing the temperature and causes a smaller rate of atomizer evaporation. In the radiation-controlled method the desired temperature could be reached very quickly, resulting in faster atomization of sample.[19]

Historically electrical parameters were used to indicate the analysis conditions for particular experiment. Filament temperature is a much more useful parameter than electrical parameters as it is independent of the instrument, but there were not convenient methods to estimate the filament temperature. However, the development of a method to accurately estimate the temperature has made it possible.

1.4. Spectral and Chemical Interference

Spectral interference arises due to the absorption of an interfering species that either overlaps or lies close to the analyte absorption wavelength. This type of interference is called background absorbance and is difficult or impossible to resolve with the monochromator. Therefore, a background correction method must be used. [8,18]

Chemical interference arises due to the formation of a thermally stable compound of low volatility with the analyte, which reduces the rate of analyte atomization.[8,18]

1.5. Reactions for Copper

The mechanism for the formation of free atoms can be by reduction of a particular nitrate or oxide by hydrogen gas or tungsten. It can also be from the evaporation or reduction of dried salts from the analyte solution and thermal dissociation of oxides.[20]

At 340 K dehydration of copper(II) nitrate occurs and as the melting point of nitrate is from 387 K-391 K one nitrate molecule is lost around 500 K. Then the copper nitrate

becomes unstable and copper oxide forms by direct decomposition of basic nitrate at 530 K.[21]

$$Cu(NO_3)_2.3H_2O \rightarrow CuO \quad (3)$$

The formation of the atomic copper can occur by any of the following mechanisms:[20]

$$CuO_{(s,l,g)} + H_{2(g)} \rightarrow Cu_{(s,l,g)} + H_2O_{(g)} \quad (4)$$

$$CuO_{(s)} + 1/2W_{(s)} \rightarrow Cu_{(s)} + 1/2\ WO_{2(S)} \quad (5)$$

$$2Cu_{(s)} \rightarrow Cu_{(l)} + Cu_{(g)} \quad (6)$$

As shown in the above chemical equations the atomic copper can be formed due to the action of the hydrogen gas in the purge gas, in reaction with the tungsten filament and solid copper. The reaction of copper with tungsten gives off different forms of tungsten oxide (W_xO_y); the ratio of x to y runs from 1:2 to 1:3. This tungsten oxide causes interference by forming a layer on the surface of the filament and the vaporized tungsten oxides block the light path to the spectrograph. [22]

Chemical modifiers like ammonium dihydrogen phosphate which forms thermally more stable complexes with the analyte. Then, the pyrolysis temperature can be raised higher to volatize organic and inorganic matrix interferences.[23] The reaction that occurs after the addition of ammonium dihydrogen phosphate is as follows:

In 0.2 % nitric acid solution -

$$Cu^{2+} + 2H_2PO_4^- \rightarrow Cu(H_2PO_4)_2 \quad (7)$$

Upon drying -

$$Cu(H_2PO_4)_2 \rightarrow CuHPO_4 + H_3PO_4 \quad (8)$$

Likely at higher temperature i.e. pyrolysis-

$$2CuHPO_4 \rightarrow Cu_2P_2O_7 + H_2O \quad (9)$$

The copper pyrophosphate is stable up to 1273 K *i.e.* the maximum pyrolysis temperature. At higher temperature than that it dissociates to give copper atoms during the atomization step. [23]

1.6. Quantitation

The ETAAS absorbance signal can be quantified in terms of the peak height or integrated area. The peak height depends on the atomization time and the rate of temperature change, with faster heating resulting in large peak height. It typically has a lower limit of detection and better sensitivity. Peak height is more dependent on the matrix present in the sample. The integrated area is dependent on the total number of atoms produced in the atomized sample. It is independent of the heating rate and also independent of the kinetics of atomization. [24]

The integrated area of the absorbance signal is directly proportional to the number density of gas phase analyte atom and can be given by the following equation (10)

$$\int A_t \, dt = k_A \, No \tag{10}$$

In the above equation k_A is the instrumental constant and *No* is the atom number density

The peak height of the absorbance signal can be approximated by equation (11)

$$A_p = k_A 2 N_o \frac{\tau_2^2}{\tau_1^2} \times \left[\frac{\tau_1}{\tau_2} - 1 + \exp(-\tau_1/\tau_2) \right] \tag{11}$$

In the above equation τ_1 is the atomization time, τ_2 is the residence time in the observation region. k_A is the collection of instrumental constants, and N_o is the atom number density. If production of atoms is very fast (small τ_1) the peak height can be approximated as $A_p \approx k_a N_o$. [24]

The integrated area or peak height can be used according to the nature of the sample being used.

1.7. Characteristic Mass and Detection Limit

According to IUPAC gold book, the characteristic mass or absolute sensitivity is the mass of analyte required to produce a peak height signal of 0.0044 A or an integrated area signal of 0.0044 A·s. [8]

According to IUPAC, the detection limit is the concentration that will give an absorbance signal three times the magnitude of baseline noise.[8]

This project investigated the concentration of copper in serum by the use of locally build compact WETAAS. As copper is one of the contaminants of drinking water, there have been few studies for concentration of copper in water by WETAAS. There are none with the complex matrix systems for copper as in serum, nor have examined the effect of interferences with WETAAS. However, these copper samples have been analyzed after various pretreatment steps such as microwave digestion and ultra filtration in a centrifuge. [3,13] This project investigated the aqueous samples of copper and serum containing copper samples for the pyrolysis and atomization conditions and for copper content in serum. All the experiments were designed without the pretreatment steps as for compact and portable WETAAS. This study also determined the detection limit and characteristic mass for copper in this instrument.

CHAPTER II

EXPERIMENTAL

The direct analysis method for copper in serum was developed on a locally built tungsten filament electro thermal atomic absorption instrument.

2.1. Instrumentation

The components of this instrument included the tungsten coil filament as an atomizer, which was extracted from a 15 V, 150 W commercially available Osram halogen display/optic lamp (Osram Xenophot 62633 HLX, Germany). The filament was connected to a commercial lamp socket (Model TP 56, Osram Sylvania) and then was housed in a glass shroud (vaporization cell) created by Chemglass. The glass shroud had two fused-silica windows arranged in a T-shaped configuration, with the dosing hole for injecting sample on the top and quartz windows on the ends. This configuration is similar to that used in other tungsten ETA systems.[9,17]

Figure 5. The Tungsten Filament and House Enclosure in the Lab.

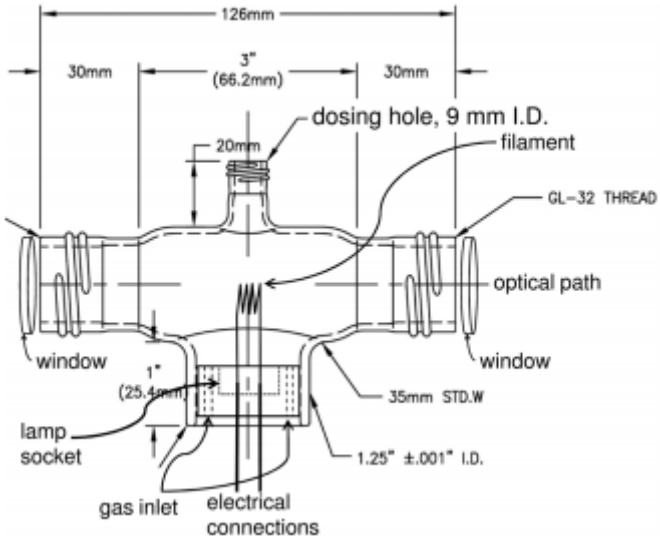

Figure 6. The Schematic Diagram of Tungsten Filament and Enclosure.[14]

As shown in the figure, the lamp socket had the inlet for the gases as well as for the electrical connections to power the filament. The support gas contained argon and hydrogen in a 90/10 ratio. The gas flow rate was maintained as 0.5 L/min with a Bel-Art meter (model no. 218751-2) adjusted at 100. Gas entered from the bottom of the shroud, then escaped through the dosing hole. The support gas helped to prevent oxidation of the filament and provided the reducing environment during the atomization step along with cooling of the glass shroud during heating cycles.[9,14]

The instrumental arrangement contained a copper hollow cathode lamp (HCL) as a light source (model no. WL 23041, Westing house - 337, USA). It was operated at 4 mA by a power supply (Oriel Corporation of America model no. 6800).[18] The HCL was followed by a 50 mm fused silica lens (NT48-294, Edmund Optics) placed on an adjustable platform (model 55651, Edmund Optics). Then the glass shroud arrangement was placed, which was followed by another 50 mm fused silica lens arranged as the previous one. The vertical and horizontal placement of the filament inside the glass shroud was adjusted with the help of screw gauge (Parker Hannifin Daedal). The initial lens focused the beam of light coming

from the HCL to a point above the filament. The later lens refocused the beam of light exiting from the window on the opposite side of the glass shroud onto the entrance slit of an ultraviolet spectrograph (Maya 2000 Pro, Ocean Optics Spectrometer, serial no. MAYP11682). The signals were recorded with Spectra Suite in strip chart mode via a Charged Coupled Device (CCD) detector with 2048 x 64 pixels. This UV spectrograph had the working range from 185 nm - 400 nm with the entrance slit width of 5 μm and resolution of 0.2 nm. The data recorded by Spectra Suite were integrated using the Grams/AI 8.0 Spectroscopy Software (Thermoelectron).

The temperature of the filament at a particular voltage was given by the voltage and current readings of a Picoscope 3425 differential oscilloscope operated at 100 Hz. The Picoscope generated a 2D plot of the readings with electrical potential difference on the y-axis and time on the x-axis, which was then converted to temperature by Grams/AI 8.0 Spectroscopy Software (Thermoelectron). Fig. 7 below shows the electrical output for current and voltage; the red signal is the reading output for current and the black one for the voltage.

The voltamperometric temperature model was based on the temperature dependence of the filament resistance. The length of pure tungsten filament '*L*', the cross-sectional area '*A*', the resistance '*R*', could be related to the electrical resistivity, ρ, as:

$$R(T)=\rho(T)\, L/A \qquad (12)$$

Using Ohm's law, the resistance is easily measured as R=V/I, where voltage is *V* and current is *I*. The *L/A* that was measured in this laboratory matched well with a previous determination as only a 7% difference was found in filaments measured 15 years apart. [17]

The voltamperometric temperature calibration shown in Fig. 8, [17] gave the equation for final fit of temperature (*T*) and resistance (*R*) for the 15 V tungsten filament, equation(13)

$$T = 23.59 + 2716 \times R^{0.8367} \quad (13)$$

As the current and voltage traces are recorded for the experiment as in Fig.7, the manipulation of these two traces results in the temperature at any point in the experiment. The highest temperature was selected for each step of WETAAS.

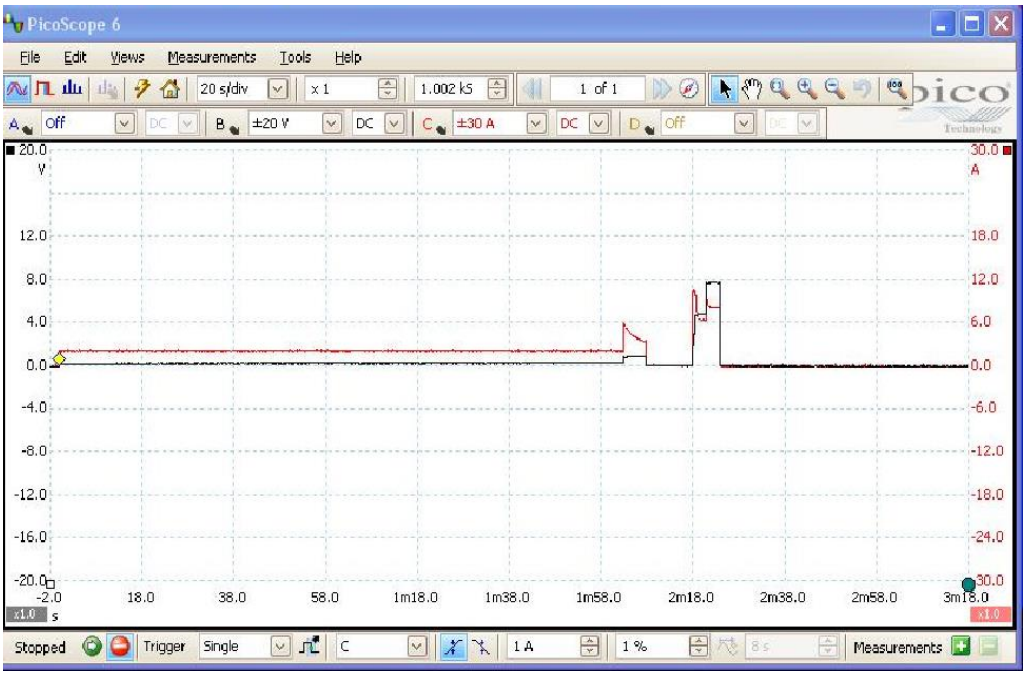

Figure 7. The Current and Voltage Traces from the Experiment

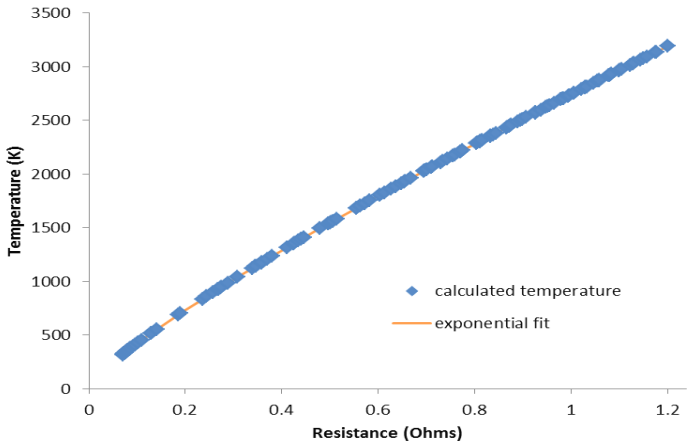

Figure 8. Calibration Curve for Temperature and Resistance

The voltage and current to the filament was controlled by a direct current (DC) power supply (model 1696, BK Precision) connected to a computer via a serial port. The current and voltages could be set accordingly with specific time for each step from 0.0 to 10.0. For this whole set of experiments the voltage mode was selected. In the voltage mode, the greater initial heating is seen due to larger current needed to reach the optimum voltage. There is a decrease in voltage at the filament relative to the power supply due to loss of voltage to overcome the resistance of the lead wires. As a result, we were careful to measure current at the base of the filament, rather than at the terminals of the power supply.

2.2. Procedure

The power supply to copper hollow cathode lamp was set gradually to reach 4 mA. The filament was inserted onto the socket and then adjusted with the help of a screw gauge. Adjustment was done so that the beam of light coming from the HCL was focused on the top of the filament and was in the center position for the entrance slit of the spectrometer. This position was termed zero position for the filament. Then the different positioning for the filament were also analyzed below the zero position. The filament was lowered below the actual zero position *i.e.* the filament was moved below the entrance slit of the spectrograph by 0.25 mm then 0.50 mm and 0.75 mm accordingly for correct positioning of the filament to get better absorbance signal. Later, the glass shroud was fitted to the socket without disturbing the beam of light. These adjustment were done with the help of the signal on the Spectra Suite software on the computer screen. The optimized position was taken as the HCL and the filament position that maximized the light throughput.

The analytical line, background, and baseline wavelengths were selected to get the time profile of them during each cycle. According to the literature, the analytical line for copper is at 324.75 nm. The background wavelength was selected as the Cu line at 323.11

nm for Cu, which is an insensitive copper wavelength. The baseline (black body) wavelength was selected at around 324.11 nm.[1] This is a point in the spectrum near the analytical line but with zero signal that will give an estimate of the amount of blackbody emission when the filament is hot. For the integration of the absorbance signal the two-line correction method was used to determine the net absorbance signal at 324.75 nm. The baseline was subtracted from both the analytical and background first to remove the blackbody from both. The background line was close to the analyte emission line and its absorbance was measured and subtracted from the total absorption to get net atomic absorption.[25] Fig. 9 shows the analytical line (green), the background line (blue) and the baseline (pink) for 10 µL of a 80 ng/mL sample.

Figure 9. The Intensity of Lines at Different Wavelengths

The BK precision power supply was set according to the required current, voltage, and time for each step as pyrolysis and atomization. The Picoscope oscilloscope was

automatically triggered by the start of the power supply for getting the current and voltage data. Lastly, before injecting the sample, support gas was turned on and was adjusted to 100 on the Bel-Art meter, which is the rate of 0.5 L/min and the connections were rechecked. All samples were 10 µL aliquots loaded each time using a 100µL adjustable volume micropipette (Eppendorf Research) via the dosing hole onto the filament surface. Once the sample was loaded on the filament, the cycle was started by clicking "Run" on the power supply, which would start the strip chart and Picoscope readings. Five replicates for each sample were performed to get the mean value and standard deviation.

There was significance of each step in the cycle as in the drying step the solid sample was left behind after evaporation of the solvent in the sample. Similarly, in the pyrolysis step the organic and inorganic matrix components of the sample were volatilized. In the pause step the filament was allowed to cool to room temperature. These steps were followed by the atomization step, which created the atomic cloud for analysis. Its temperature should be high enough to atomize all the atoms. Then finally the cleaning step removed the sample residue on the filament and was generally done with higher voltage than the atomization step.

The conditions for the pyrolysis and atomization steps were determined by plotting the data, keeping one constant and varying the other and vice-versa. The calibration curve was plotted for different concentrations of similar samples to get the desired pattern. For the determination of the copper content in a serum sample, the standard addition method was applied. The power supply values for the different steps in a typical analysis are shown in the table below:

Table 1. Electrothermal Atomization Steps

Method	Variant	Time
Dry	2 A (493 K)	125 secs
Pyrolysis	1.6 V (1257 K)	5 secs
Pause	0A (298 K)	10 secs
Atomize	5 V (2141 K)	3 secs
Clean	7 V (2583 K)	3 secs

The data from Spectra Suite software were converted to absorbance, background subtracted and integrated using the Grams/AI software to get the mean area and peak height of the waveform. The voltage and current data from the Picoscope was solved for the temperature using a previously developed calibration. These data were then plotted in Microsoft Excel to get the optimum pyrolysis and atomization voltage and the values for copper in serum. The Limit of Detection (LOD) and Quantification for copper concentration were done according to the Calibration Curve Method and the Standard Addition Method respectively.

2.3. Sample Preparation

All the samples were prepared in 0.2 % (v/v) nitric acid solution that was diluted from trace metal grade nitric acid (Lot No. 1110070, Fisher Scientific, Assay 67-70%). The 5.7 mL of the nitric acid was diluted to 2000 mL with Type 1 water (model 823752, Millipore). This solvent was used for copper sample conservation, as the solutions should be acidified to pH value < 1.5 with nitric acid to keep metal ions in solution.

A 8 mg/L copper stock solution was prepared by diluting 2 mL of 1000 mg/L of copper in 2% nitric acid (#SC194-500, Lot No- 910371-24, Fisher Scientific) to 250 mL with

0.2% (v/v) nitric acid solution. All the standards for copper were diluted from this copper stock solution.

A 2% ammonium phosphate modifier was prepared by using 2 g of ammonium dihydrogen phosphate (trace metal basis 99.999%, Lot no. A0335836, Acros Organics) dissolved in 0.2% nitric acid solution to make 100 mL. The modifier was used in some experiments to stabilize copper at higher temperature. The 2% ammonium phosphate modifier was diluted 10 times from the standard solution to obtain 0.2% modifier.

A 30,000 mg/L sodium chloride (NaCl) solution was prepared from 3.0 g sodium chloride (Assay 99.99%, Lot no- L-11621, Fisher Chemical) in 100 mL of 0.2% nitric acid solution. It was diluted in each standard solution to get 900 mg/L sodium chloride, which resembles the sodium and chloride concentrations in human blood.[1]

A 0.1% (w/v) solution of Triton X- 100 in Type 1 water was used as a surfactant as per the literature[26] to avoid the coagulation of protein in serum with low matrix interference. It was used in the samples where serum was present and in the aqueous standard solution for standard addition. The dilution for the samples was 10 parts of 0.1% (w/v) Triton X-100 in 100 parts of the solution.

The different concentration standard solutions were prepared by dilution of 8 mg/L copper stock solution in 0.2% nitric acid solution. The experiments were designed for different samples with modifier, without modifier, with sodium chloride, with sodium chloride and modifier. All the dilutions were performed with volumetric glassware such as volumetric pipettes and volumetric flasks.

After finding the appropriate conditions for each of the steps the horse serum (Sigma, #H1270-500 mL, donor herd, sterile filtered) sample was used to analyze the copper in it. The horse serum was gravimetrically diluted in a 1:5 ratio with the known concentration of

copper standard solution in semi-micro weighing balance (Satorius, model - CPA 225D). The copper concentration in serum was determined with standard addition tool, where the aqueous and the serum samples were made with 5 parts of known concentration of standard copper solution and 1 part of 0.2% nitric acid solution and 1 part of horse serum respectively.[27]

CHAPTER III

RESULTS AND DISCUSSION

3.1. Filament Positioning

The effect of the position of the filament relative to the entrance slit of the spectrograph was evaluated. The top surface of the filament was positioned at different heights from the bottom of the entrance slit of the spectrograph. The "zero position" was the coincidence of the top of the filament with the bottom of the entrance slit. The filament was placed 0.25, 0.50 and 0.75 mm below the entrance slit by using the micrometer adjustment of the translation stage holding the filament. A 40 ng/mL copper solution was used as the sample to assess changes in the absorbance as a function of filament height.

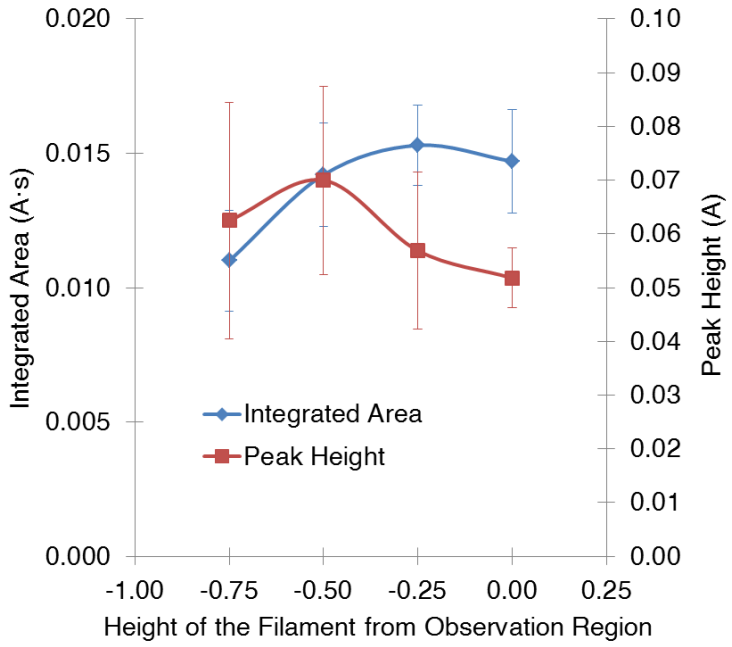

Figure 10. Positioning of Filament and Their Corresponding Values.

As shown in Fig.10 the filament positioned 0.25 mm below the light path maximized the recorded integrated area with less error than the zero position, 0.50 mm and 0.75 mm below the zero position. The peak height did not show a definite pattern for the determination

of the filament positioning, The integrated data showed that area increased at 0.25 mm below the zero position of the filament as there were more copper atoms in the path of light than with the filament at other positions. The result suggests that as the molecular forms of copper vaporized from the surface of the filament and had more time to stay in the high temperature region, they were increasingly dissociated to copper atoms when they reached the observation region of the spectrograph. Consequently, 0.25 mm below zero was selected as the filament position for all future experiments.

3.2. Conditions for Pyrolysis and Atomization

The optimum conditions for pyrolysis and atomization were investigated for copper in variety of solutions. For determining the pyrolysis condition, atomization voltage was kept constant and for the atomization condition pyrolysis was kept constant.

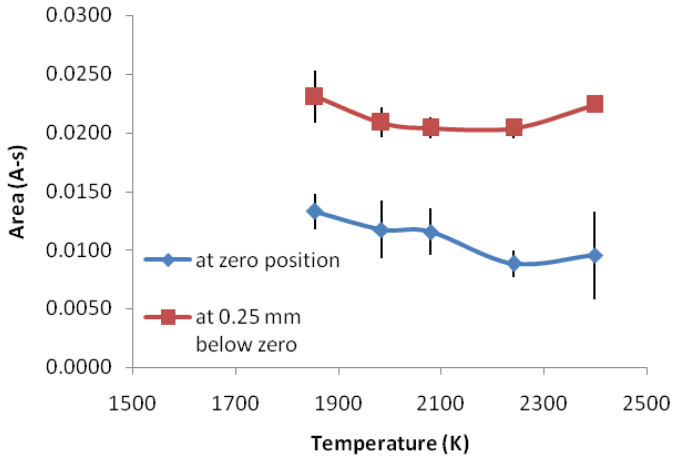

Figure 11. Comparing Atomization at Filament Position Zero and 0.25 mm Below Zero

The best conditions for atomization were determined by measuring the integrated copper signal at several atomization temperatures, as shown in Fig.11. The integrated areas recorded at the zero position and 0.25 mm below the zero position were compared to get the atomization condition. Only area was considered because the peak height had no distinctive

result. Fig.11 shows that there was an increase in the atomization integrated area as the position of filament was lowered.

In Fig.11, a 40 ng/mL copper sample was analyzed through different atomization voltages of 4.0, 4.5, 5.0, 5.5 and 6.0 V with the pyrolysis condition constant at 1.8 V. The best temperature was selected in the flatter region of the plot as the higher temperature did not follow the pattern. Similarly, that particular temperature region should have better precision within its areas. The atomization temperature of 2073 K, corresponding to 5 V, was the best atomization condition and this agreed with the temperature range of 2000 K to 2600 K found in the literature.[1,28]

This atomization temperature was used to determine the best pyrolysis temperature by measuring the integrated absorbance signal at several pyrolysis conditions. A 80 ng/mL copper sample was analyzed through different pyrolysis voltages as from 1.2 to 1.8 V in 0.1 V increments with the atomization condition constant at 5 V.

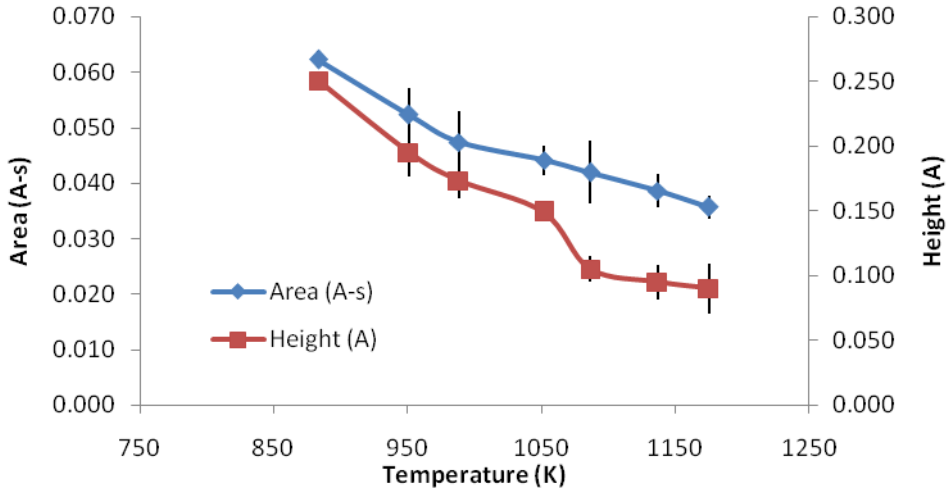

Figure 12. Pyrolysis Area and Peak Height at Atomization Voltage of 5 V.

In the above Fig.12 as the pyrolysis temperature corresponding to different voltages increased the mean area and peak height gradually decreased, which shows that there was a

loss of copper during pyrolysis as the temperature increased. According to Fig. 12 the maximum pyrolysis temperature was 900 K, corresponding to a voltage of 1.2 V. Similarly, the copper sublimes around 1400 - 1600 K according to the activation energy of about 337 $KJmol^{-1}$, so the pyrolysis temperature should not exceed 1400 K.[24] At 900 K the curve had the highest possible area and height as well as better precision than others.

After determining the pyrolysis and atomization conditions suitable for an aqueous solution, the best working condition for the modified aqueous solution was also determined. A 80 ng/mL modified copper sample was used for this determination. These readings were taken at 0.25 mm below the zero position of the filament.

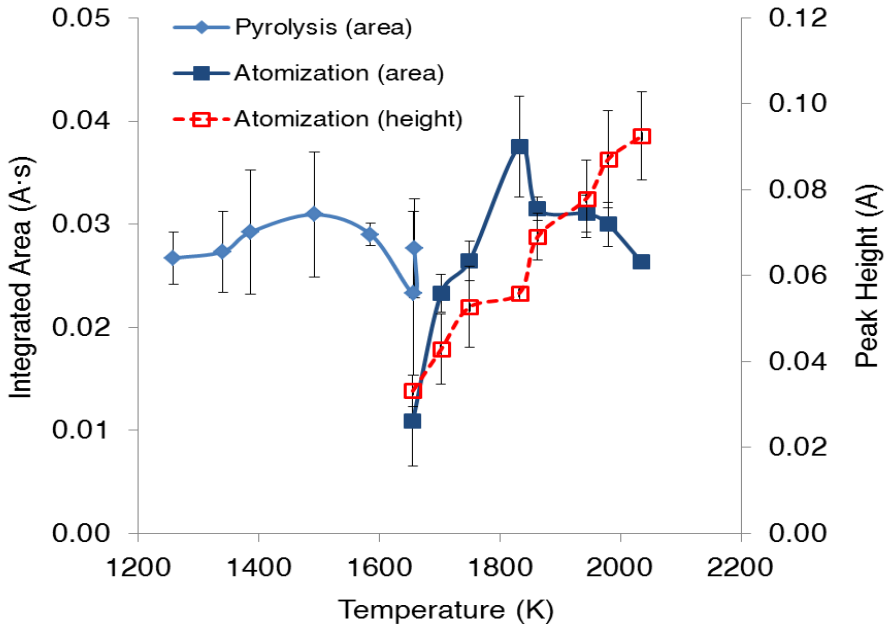

Figure 13. The Pyrolysis and Atomization Conditions with Added Matrix Modifier.

In Fig. 13 the pyrolysis area shows that after addition of the modifier the temperature for pyrolysis could be increased without loss of analyte in this step. The above plot shows the maximum pyrolysis voltage at 2.2 V, which corresponds to 1492 K, as after that the result started to become less reproducible. Similarly, from the atomization integrated area the temperature at 1953 K, corresponding to 5 V, was the best working condition for atomization

as the area started to decrease after this. The peak height for atomization kept on increasing with increasing atomization temperature. This is the expected result since peak height is a function of the filament heating rate, which increases with voltage.

The conditions for pyrolysis and atomization voltages were determined with and without ammonium dihydrogen phosphate as modifier in samples containing horse serum. The samples were 160 ng/mL copper aqueous solutions with and without modifier mixed in a 5:1 ratio with serum.

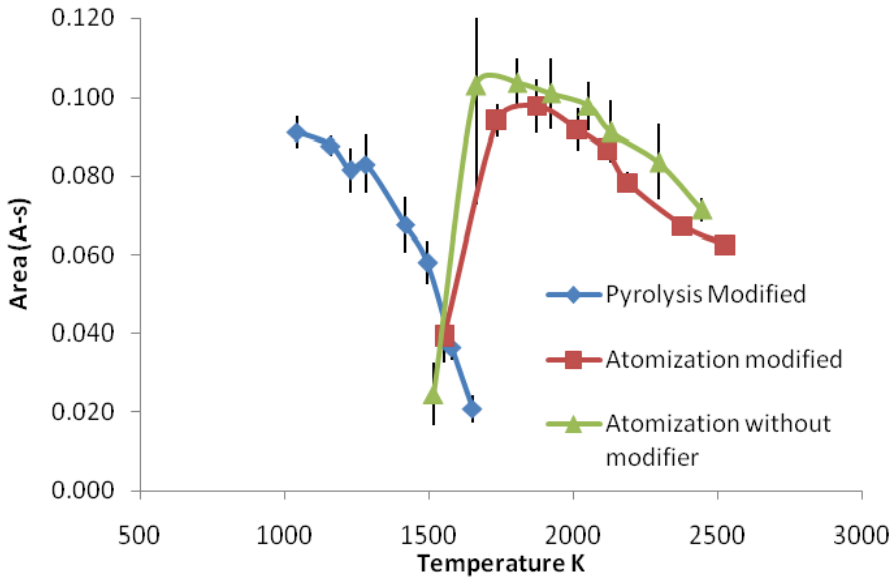

Figure 14. The Pyrolysis and Atomization Area With and Without Modifier.

In Fig.14 the curve for pyrolysis area of the modified sample shows that the pyrolysis area decreased as the temperature for pyrolysis increased. The maximum pyrolysis voltage selected was the first one at 1.2 V, corresponding to 1043 K. The modified and unmodified area for atomization were similar. The selected atomization voltage was 5 V corresponding to 2190 K. This curve showed that when there is serum in the sample in the form of interference then ammonium dihydrogen phosphate as modifier did not stabilize the copper. As in Fig. 14, (the pyrolysis curve for the modified sample) serum itself acted as a modifier.[1]

According to the literature, the maximum pyrolysis temperature for copper should be around 1273 K for a complex matrix system like serum. As 1.2 V (900 K) was too low without the modifier and 2.2 V (1492 K) was too high with the modifier for pyrolysis, an intermediate temperature was examined. The pyrolysis voltage for the modified and unmodified 80 ng/mL copper sample was varied from 1.4 V to 1.9 V as in previous experiments. The conditions matching the literature were about 1.5 V and 1.6 V, *i.e.* their temperature were around 1273 K. Then using 1.5 V and 1.6 V as the pyrolysis condition the investigation for best condition for pyrolysis time was performed from 5 seconds to 10 seconds for both modified and unmodified copper samples.

The selection for best voltage and time with and without modifier was done by a comparison of the two experimental means using the t-test. For the comparisons t-critical was 2.31. The t-test in Table 2 shows that at the 95% confidence interval the 1.5 V and 1.6 V pyrolysis results were not different and that doubling the lengths of pyrolysis did not have a significant effect. The addition of modifier did not have a significant difference either. The results indicate that 5 seconds was enough to volatize the matrix material from the system and there are not any kinetic problems with the short pyrolysis time. For subsequent analyses, 1.6 V for 5 seconds and without adding modifier was chosen as the best condition for pyrolysis.

Table 2. Values from Statistical Analysis.

Parameters	S_{pooled}	t-value
1.5 V and 1.6 V	0.0018	1.70
5 secs and 10 secs	0.0057	0.78
Modified and Unmodified at 1.6 V for 5 secs	0.014	0.94

A 80 ng/mL copper solution with 900 mg/L of sodium chloride as an interference in it was analyzed to determine the best pyrolysis and atomization temperatures. Similarly, the same concentration of copper and sodium chloride was analyzed with ammonium dihydrogen phosphate as the modifier.

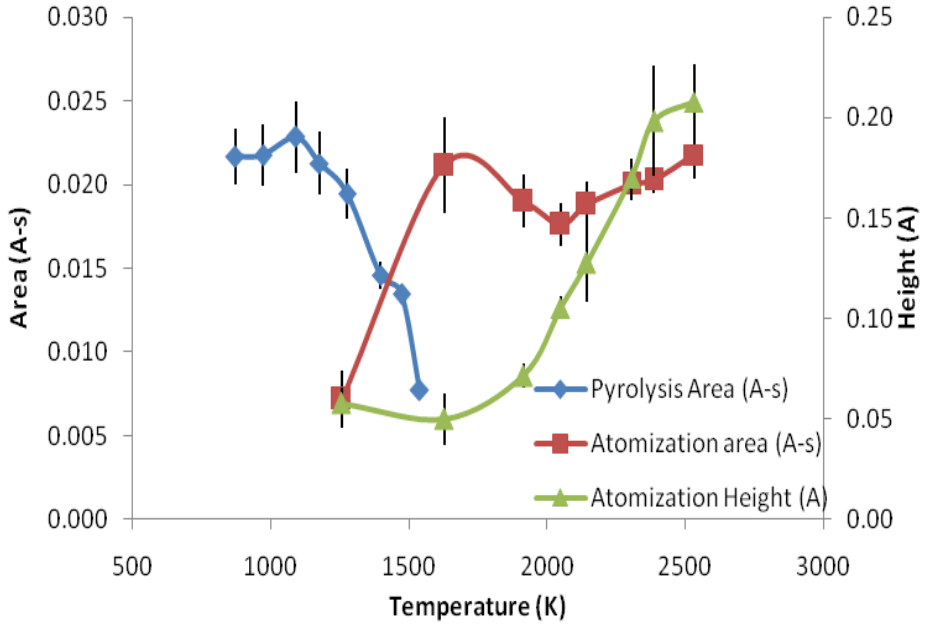

Figure 15. Aqueous Copper Solution with NaCl as Interference

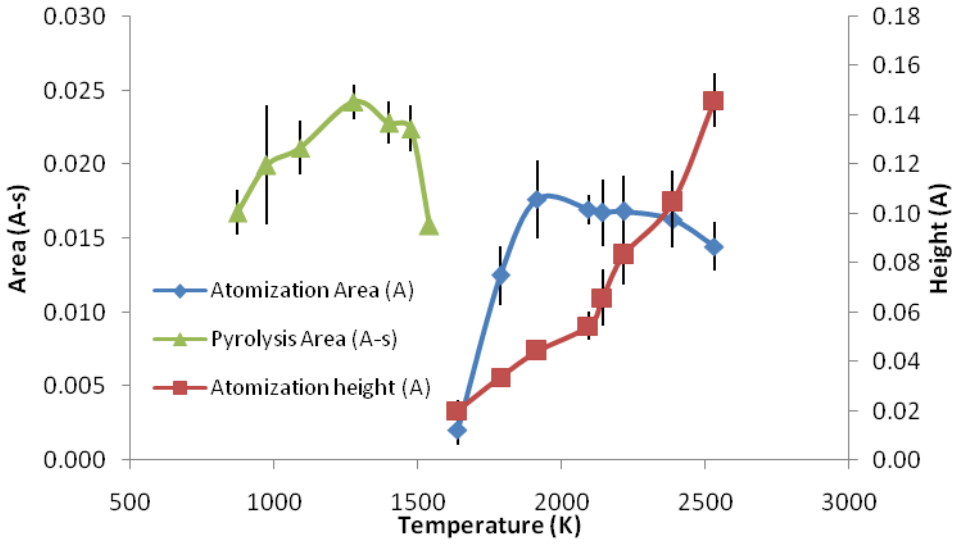

Figure 16. Modified Copper Aqueous Solution with NaCl as Interference

In Fig. 15 the pyrolysis and atomization curves with addition of NaCl as interference in an aqueous copper solution is shown. The pyrolysis voltage was varied from 1.0 to 2.2 V in 0.2 V increments. The mean area for pyrolysis decreased after 1.2 V (1000 K), which shows that there was a loss of copper after that temperature. Then the atomization voltage was varied from 2.5 to 6.0 V in 0.5 V increments. The curve for the mean area and peak height for atomization remained flat around 5 V (2307 K) with better precision within areas. Therefore, the pyrolysis condition of 1.2 V and atomization condition of 5 V was best for aqueous copper solution with sodium chloride as interference. There was not much effect of the sodium chloride as interference in the aqueous copper solution, as the pyrolysis and atomization conditions were similar comparing the conditions obtained for the aqueous copper only solution in Fig.11 and Fig. 12. Similarly, Fig.16 shows the pyrolysis and atomization curves for the modified aqueous copper solution with NaCl as interference. The pyrolysis voltage varied from 1.2 to 2.4 V in 0.2 V increments. The mean area for pyrolysis decreased after 2.2 V (1482 K), which shows that there was a loss of copper after that temperature. Then the atomization voltage was varied from 2.5 to 6.0 V in 0.5 V increments. The curve for mean area and peak height for atomization remained flat around 5 V (2218 K) with better precision within areas. This pyrolysis and atomization condition matches the one for the aqueous solution with modifier in Fig. 13.

These pyrolysis and atomization conditions obtained for phosphate modified and unmodified aqueous copper solutions proved that there is not much difference in the matrix after addition of sodium chloride as interference. This is true according to the literature, as it stated there would not be any effect of interference up to 30 g/L of NaCl in copper solution.[1]

3.3. Quantitation

The pyrolysis and atomization conditions for aqueous solution were used to determine the limit of detection using a calibration curve. Only the mean area was considered since the peak height had no distinctive result.

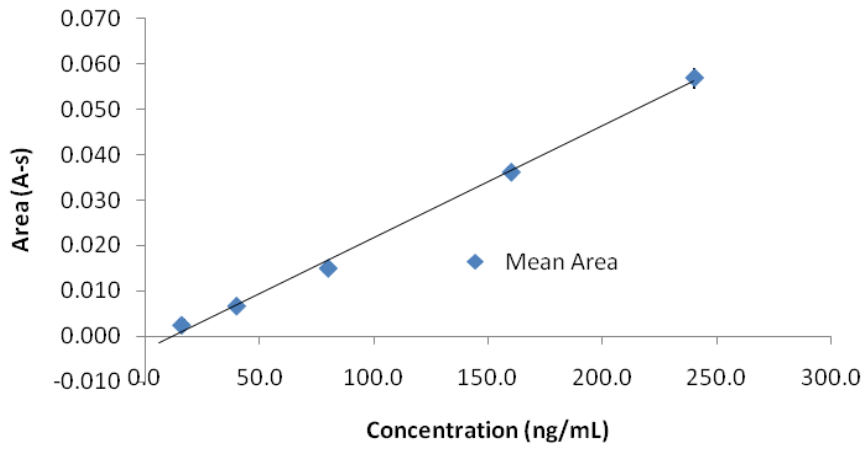

Figure 17. Calibration Curve for Aqueous Copper Solution.

The aqueous calibration curve in Fig.17 gave the limit of detection as 28.9 ng/mL and the absolute sensitivity of 0.06 ng from the integrated area of the absorbance.

A set of aqueous copper standards were made and diluted in a 5:1 ratio with 0.2% nitric acid solution. Then these aqueous copper samples were analyzed to determine the mean area and peak height. The calibration curve was plotted for aqueous copper solution as shown in Fig.18. Similarly, the aqueous copper standards were diluted with horse serum in a 5:1 ratio and the calibration curve was plotted as shown in Fig.19. A standard addition determination was performed for the concentration of copper in horse serum.

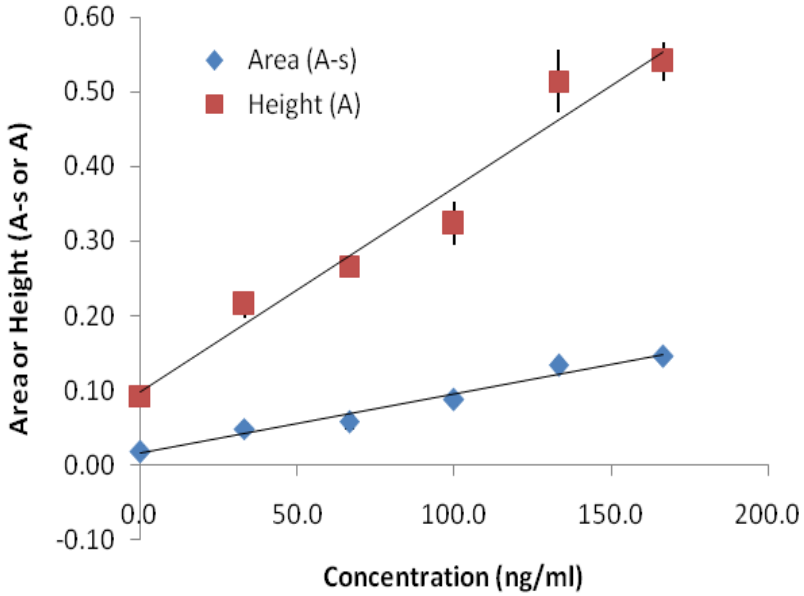

Figure 18. Calibration Curve for Aqueous Solution at 1.2 V.

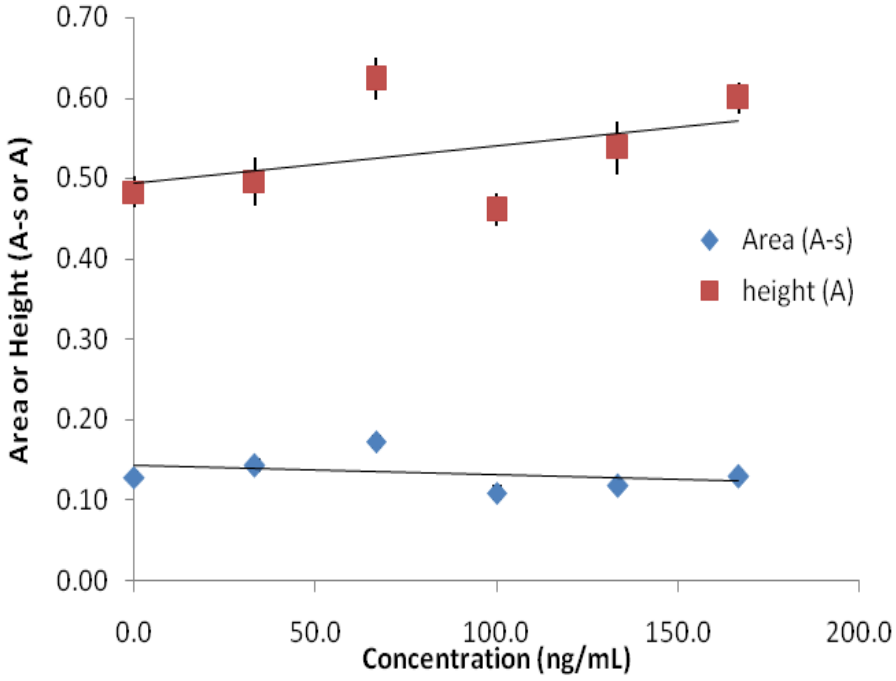

Figure 19. Calibration Curve for Serum Containing Sample at 1.2 V.

Table 3. Results from Calibration Curve at 1.2 V for Pyrolysis Condition

Analysis	Aqueous Area Results	Aqueous Height Results	Serum Area Results	Serum Height Results
Slope	0.00079	0.0027	-0.00011	0.00047
R-squared	0.99	0.96	0.096	0.19
Intercept	0.015	0.097	0.14	0.49
Limit of Detection	28.9ng/mL	42.5 ng/mL	-	-
Absolute Sensitivity	0.14 ng	0.34 ng	-	-
Content of Copper	-	-	not possible	1061 ± 3237 ng/mL

The calibration curves shown in Fig.18 and Fig.19 used 1.2 V as the pyrolysis voltage and 5V as the atomization voltage. The aqueous curve had a low limit of detection for both area and peak height. The content of copper obtained from integrated area was not acceptable for the concentration of copper in serum. No results could be obtained from the peak height analysis as it had negative slope for the standard addition as the background absorbance was too large.

The calibration results in Table 3 suggested that the pyrolysis conditions suitable for aqueous samples were inappropriate for the serum containing samples as there was a large matrix interference. Pyrolysis at 1000 K (1.2 V) was not enough to volatilize all of the organic and inorganic matrix. According to the literature for the analysis of copper in GFAAS the pyrolysis should be carried out at around 1273 K (1000 ºC) for serum containing samples.[1]

As 1.2 V did not work as a pyrolysis voltage for the serum containing sample the ammonium dihydrogen phosphate as matrix modifier was added to the copper-containing aqueous solutions and the serum containing samples. The samples for analysis were prepared

similarly in a 1:5 ratio of serum to the aqueous standards. This time the higher pyrolysis voltage (2.2 V) found for the phosphate modified samples was used.

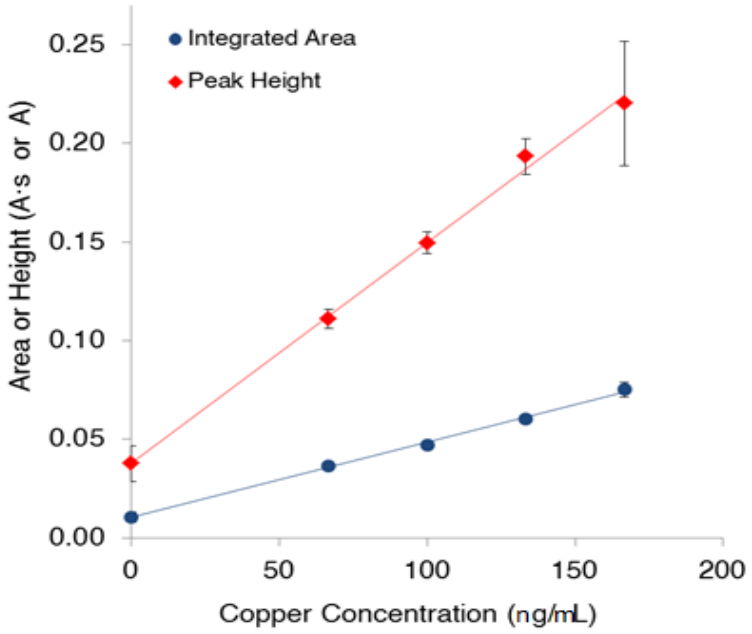

Figure 20. Aqueous Calibration Curve at 2.2 V as Pyrolysis Condition

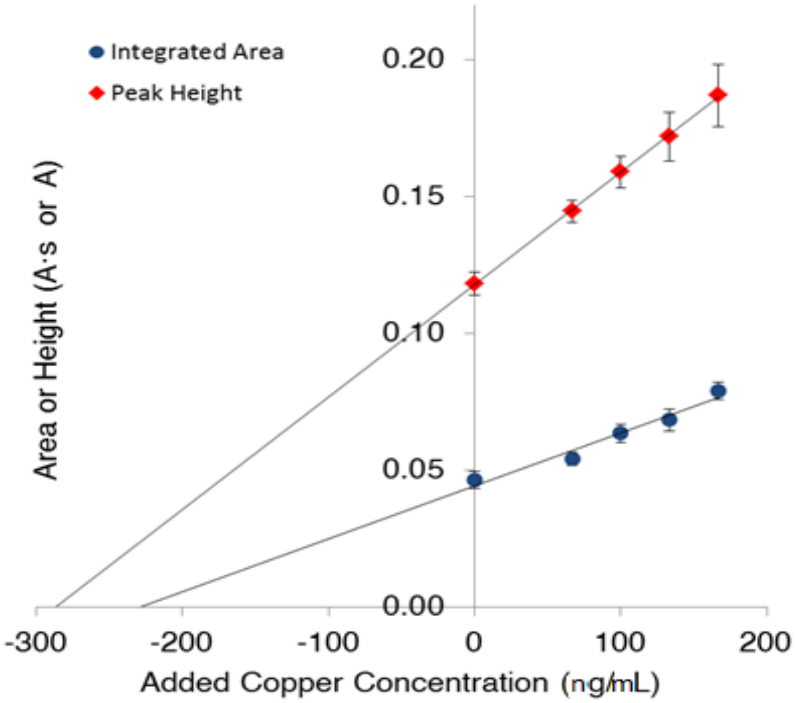

Figure 21. Serum Containing Sample Calibration Curve at 2.2 V as Pyrolysis Condition

Table 4. Results from Calibration Curve at 2.2 V as Pyrolysis Condition

Analysis	Aqueous Area Results	Aqueous Height Results	Serum Area Results	Serum Height Results
Slope	0.00038	0.0011	0.00019	0.00041
R-squared	0.99	0.99	0.96	0.99
Intercept	0.010	0.037	0.044	0.12
Limit of Detection	9.9ng/mL	11.9 ng/mL	-	-
Absolute Sensitivity	0.15 ng	0.29 ng	-	-
Content of copper	-	-	229 ± 117 ng/ml	286 ± 16 ng/mL

Table 4 shows that limit of detection from the aqueous solution was very low but the copper content in serum detected was higher than expected. This suggested that there was a loss of analyte during pyrolysis, giving less integrated area and height and resulting in the calibration curve with incorrectly low sensitivity.

As both 1.2 V and 2.2 V were not able to give the desirable concentration of copper in serum, the statistically determined condition for pyrolysis at 1.6 V for 5 sec was used for a unmodified aqueous solution.

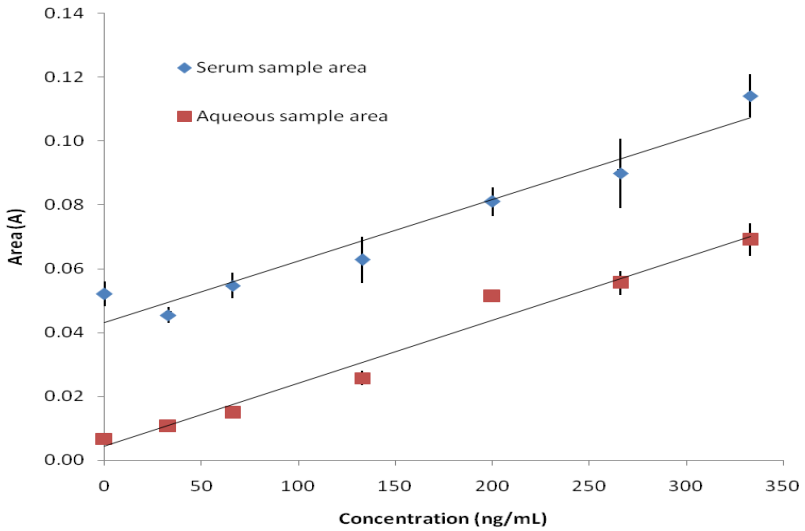

Figure 22. Calibration Curve for Aqueous and Serum Samples from WETAAS

The samples for aqueous and serum containing samples were prepared in a 5:1 ratio as before.

Table 5. Results from Calibration Curve at 1.6V as Pyrolysis Condition for WETAAS

Analysis	Aqueous Solutions Results	Serum Sample Results
Slope	0.00019	0.00019
R-squared	0.97	0.95
Intercept	0.0043	0.043
Limit of Detection	66.2 ng/mL	-
Absolute Sensitivity	0.0036 ng	-
Content of copper	-	173 ± 74 ng/mL

The aqueous and serum containing samples in Fig. 22 had similar slopes, which showed that they had little interference. Table 5 shows that the limit of detection was low and the content of copper was within the expected range. The sensitivity was good too.

This result was compared with the FAAS analysis of copper in serum. The samples were the same as those used in the WETAAS determination. The quantitation was done with standard addition.

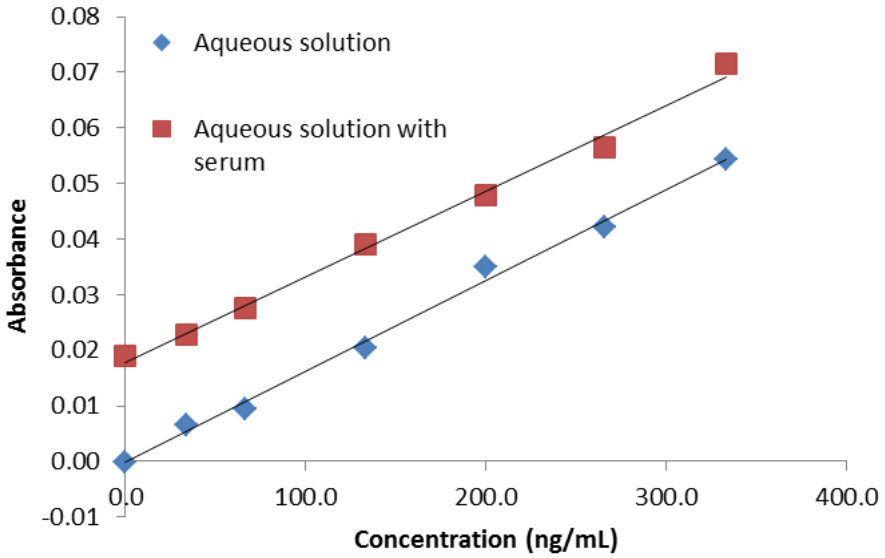

Figure 23. Calibration Curve for Aqueous and Serum Containing Sample from FAAS.

Table 6. Results from Calibration Curve of FAAS

Analysis	Aqueous Solutions Results	Serum Samples Results
Slope	0.00016	0.00015
R-squared	0.99	0.99
Intercept	0.00009	0.02
Limit of Detection	29.5 ng/mL	-
Characteristic Concentration	0.26 ng	-
Content of serum	-	115 ± 28 ng/mL

The calibration curve in Fig. 23 shows both the aqueous and serum containing sample had similar slopes, which showed this process as matrix independent. Table. 6 shows that the limit of detection was low and the content of serum was within the expected range.

The copper content of serum as determined by standard addition was added to the concentration of copper in the aqueous standards and the results replotted as shown in Fig. 24 and Fig 25. For both the FAAS and WETAAS data, the two sets of data are nearly colinear, indicating good matrix independence.

The results obtained for the copper content from WETASS and FAAS for horse serum in Table 5 of 173 ± 74 ng/mL and Table 6 of 115 ± 28 ng/mL.

Copper content in horse serum by WETAAS was 865 ng/mL i.e. 13.61 μmol/L as per 1:5 dilution of sample. t-statistics for the comparison of mean values of FAAS and WETAAS was t=5.0 which stated that these two averages were not statistically equivalent.

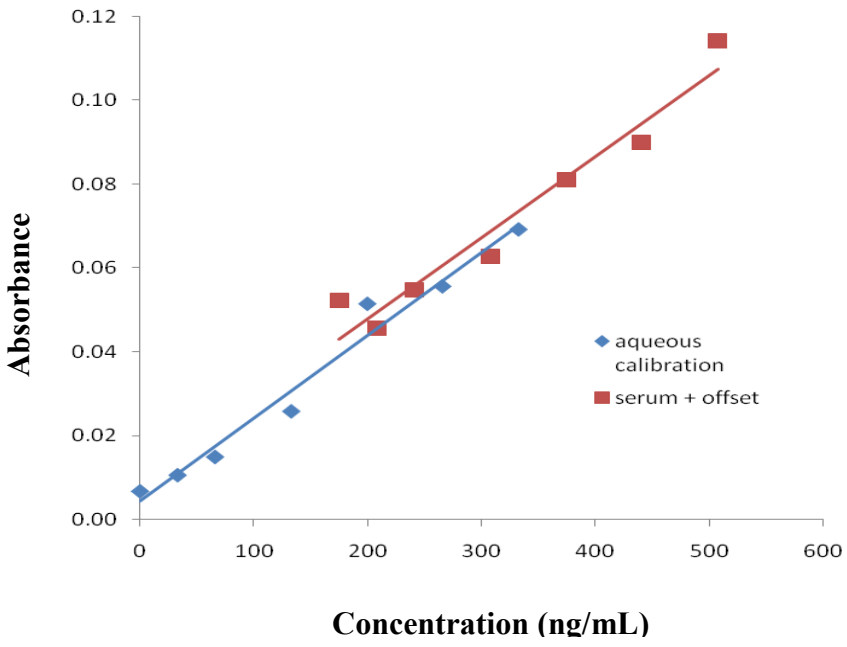

Figure 24. Replotted Data of Copper in Serum and Aqueous Solution for WETAAS

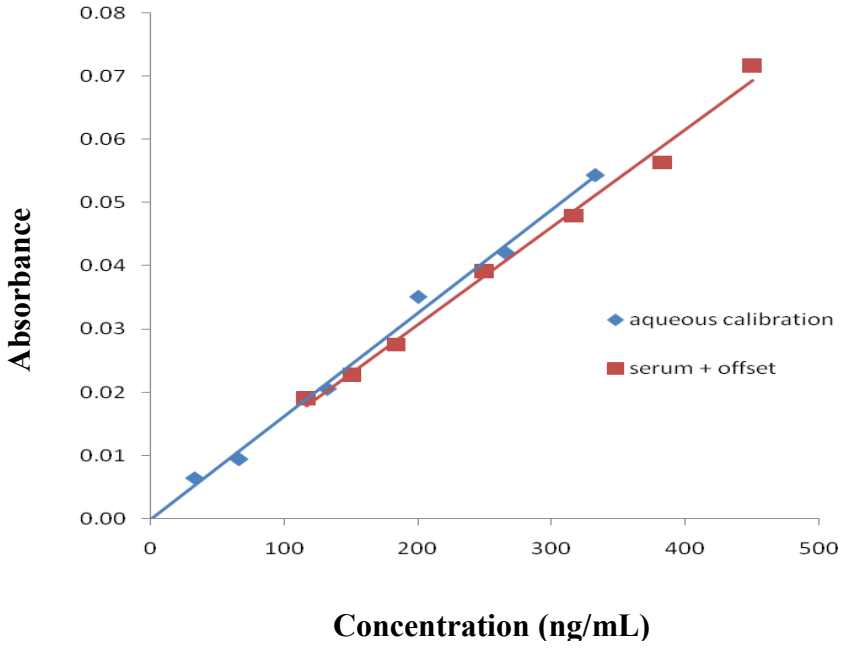

Figure 25. Replotted Data of Copper in Serum and Aqueous Solution for Flame AAS

CHAPTER IV

CONCLUSIONS

The different experimental conditions for determining the concentration of copper in horse serum and aqueous samples were investigated. A locally build compact and inexpensive tungsten filament atomic absorption spectrometry instrument was used for atomization studies and method development.

The positioning of the filament in the light path played an important role for the enhancement in the absorbance signal from atomic vapors of the analyte. A filament position 0.25 mm below the zero position was found to give the greatest atomic absorption signal.

The pyrolysis and atomization conditions were determined using the absorbance versus temperature plot for several types of solutions. The quantitation was better with integrated peak area for samples with a complex matrix as it is independent of heating rate and the kinetics of reaction. Peak height is highly sensitive since the response using height as the measurement has larger slope but did not improve the Limit of Detection (LOD) due to a smaller signal to noise ratio and height results suffer from poorer Relative Standard Deviation (RSD).

The use of ammonium dihydrogen phosphate as a matrix modifier was effective at elevating the maximum pyrolysis temperature for aqueous copper solutions. The modifier was also effective for copper samples containing a large concentration of sodium chloride as an interference. However, the matrix modifier had little effect on samples containing horse serum as an interference. The lack of modifier effect in serum-containing samples indicates that copper is not driven toward a copper-phosphate species in the presence of serum. The seru-containing samples also did not behave like aqueous copper samples and required a significantly higher pyrolysis temperature to achieve adequate quantitation. Horse serum has

a unique behavior as it acts as an interference removing the effects of the phosphate modifier, and as its own modifier, elevating the maximum pyrolysis temperature of copper relative to aqueous solutions.

The pyrolysis and atomization conditions for the aqueous copper solution was found to be 1.2 V (900 K) and 5 V (2073 K) respectively. Similarly for the modified aqueous copper samples the pyrolysis condition increased to 2.2 V (1492 K). Then the optimum pyrolysis condition for serum containing copper samples was 1.6 V (1273 K) for 5 sec at the same atomization condition as the aqueous copper samples.

The serum containing samples were prepared in a 1:5 ratio with copper standards. The copper concentration in serum was determined by calibration against aqueous copper standards and standard addition with serum-containing samples. The results obtained with the aqueous copper standards had a detection limit of 66.2 ng/mL and the absolute sensitivity was 0.0036 ng. The concentration of copper in horse serum was 173±74 ng/mL as determined by standard addition. As the serum sample was prepared by dilution in a 1:5 ratio with the aqueous standard solution, this results in 865 ng/mL, *i.e.* 16 µmol/L in agreement with the concentration of copper in horse serum as given in the literature.[4,5] The result was validated by flame AAS. In both WETAAS and FAAS, the aqueous and serum containing samples were collinear signifying these methods are matrix independent.

To completely understand the unusual behavior of copper atomization on a tungsten filament atomizer, further studies are needed. A detailed study of the reactions in the decomposition of copper nitrate to vaporized copper atoms should be investigated with the help of other methods such as thermogravimetric analysis. The reactivity of copper in the presence of serum on a tungsten surface needs to be better understood in order to identify candidates for improved matrix modifiers.

REFERENCES

[1] Welz, B.; Sperling. Atomic Absorption Spectrometry, 3rd ed.; Wiley-VCH, **1999**; pp 500-502.

[2] Ali, S.F.; Imtiaz, N.; Mehdi, S; Asif, M. Determination of Copper Concentration in Human Blood Serum by Using Flame Atomic Absorption Spectroscopy (FAAS). *ICEEPS*. **2012**, 140-142.

[3] Salido, A.; Jones, B.T. Simultaneous Determination of Cu, Cd and Pd in Drinking - Water using W-Coil AAS. *Talanta*. **1999**, 50, 649-659.

[4] Nazifi, S; Rategh,S. Haemoglobin Types and Blood Concentrations of Haemoglobin, Copper, Ceruloplasmin and Iron in Adult Caspian Miniature Horses. *Revue Med. Vet.* **2005**, 156, 50-52.

[5] Rad, P.A.; Hassanpour.A.; Mashayekhi. M. Comparative Study of Serum Zinc, Copper and Selenium in Horses with Strangles and Healthy Horses. *European Journal of Zoological Research*. **2013**, 2(5), 67-74.

[6] Malavolta, M.; Giacconi, R.; Piacenza, F.; Santarelli, L.; Cipriano, C.; Costarelli, L.; Tesei, S.; Pierpaoli. S.; Basso, A.; Galeazzi, R.; Lattanzio, F.; Mocchegiani. E. Plasma Copper/Zinc Ratio: an Inflammatory/Nutritional Biomarker as Predictor of all-cause mortality in elderly population. *Biogerontology*. **2010**, 11, 309-319.

[7] Cao, Y.; Skaug, M.A.; Anderson, O.; Aaseth, J. Chelation Therapy in Intoxications with Mercury, Lead and Copper. *J Trace Elem Med Biol*. **2014.**

[8] Beaty, D.R.; Kerber. D. J. Concepts, Instrumentation and Techniques in Atomic Absorption Spectrophotometry, *Perkin-Elmer Corporation*, Norwalk, CT, USA, **1993.**

[9] Gu, J.; Donati, G.L.; Young, C.G.; Jones, B.T. Continuum Source Tungsten Coil Atomic Fluorescence Spectrometry. *Applied Spectroscopy*. **2011**, 65, 382- 386.

[10] Welz, B.; Sperling, M. Atomic Absorption Spectrometry. John Wiley and Sons. **2008**.

[11] Almeida, A.A.; Lima, J.L.F.C. Optimized Conditions and Analytical Performance for the Determination of Cu in Serum and Urine Samples using GFAAS Procedure. Atomic Spectroscopy - Norwalk Connecticut. **2006**, 22(3), 324-330.

[12] Salman, M. Electrothermal Atomic Absorption Spectrometry Behavior of Cadmium without/with Spiral Tungsten Filaments as Platform Technique as its Application. *Der Pharma Chemica*. **2012**, 4(6), 2169-2177.

[13] Zhou, Y.; Parsons, P.J.; Aldous, K.M.; Brockamn, P.; Slavin, W., Atomization of lead from whole blood using novel tungsten filaments in electrothermal atomic absorption

spectrometry. J. *Anal. At. Spectrum*. **2001**, 16, 82-89.

[14] Navarre, E.C.; Bright, L.K.; Osterage, A.; Lada, B. Development of an N-Methyl Pyrrolidone based Method of Analysis for Lead in Paint. *Anal. Methods*. **2012**, 4, 4295-4302.

[15] Wagner, K.A.; Levine, K.E.; Jones, B.T. A Simple Low Cost, Multielement Atomic Absorption Spectrometer with a Tungsten Coil Atomizer. *Spectrochimica Acta Part B*. **1998**, 1507-1516.

[16] Donati, G.L; Pharr.K.E.; Calloway, C.P; Nobrega, J.A; Jones, B.T. Determination of Cd in Urine by Cloud Point Extraction- Tungsten Coil Atomic Absorption Spectrometry. *Talanta*. **2008**, 76, 1252-1255.

[17] Navarre, E.C.; Wallace, P. A Nonequilibrium Approach to Temperature Calibration for Tungsten Filament Atomic Spectrometry. *Spectroscopy Letters*. **2014**, 47, 314-323.

[18] Skoog, D.A.; Holler, F.J.; Nieman. T.A. Atomic Absorption and Atomic Flourescence Spectrometry. *Principles of Instrumental Analysis*, 9, 5th Ed, **1998**, 206-230.

[19] Montaser, A.; Crouch, S. R. New Methods for Programmed Heating of Electrically Heated Nonflame Atomic Vapor Cells. *Anal. Chem.* **1975**, 47(1), 38-45.

[20] Krakovska, E.; Remeteiva, D. Tungsten Atomizer- Theory of Atomization Mechanism of some Volatile Analytes. *J.Anal. Chem*., **2000**, 366, 127-131.

[21] L'vov, V.B.; Noichis.V.A. Mechanism of Thermal Decomposition of Hydrated Copper Nitrate in Vacuo. *Spectrochimica Acta Part B: Atomic Spectroscopy*. **1995**, 50 (12), 1459-1468.

[22] Santos, D. M.; Luccas, P. O.; Nobrega, J. A.; Cavalheiro, E. T. G. Thermogravimetric investigations on the mechanism of decomposition of Pb compounds on a tungsten surface.*Thermochimica Acta.* **2000,** 362, 161-168.

[23] Krakovska,E.; Remeteiova, D. Tungsten Atomizer - Action of Modifiers. *Spectrochimica Acta Part B*. **2003**, 1507-1513.

[24] Sturgeon. R. E, Chakrabarti, C. L, Maines.S, Bertels. P. C. Atomization in Graphite-Furnace Atomic Absorption Spectrometry-Peak Height Method vs. Integration Method of Measuring Absorbance. Carbon Rod Atomizer 63. *Analytical Chemistry*. **1975**, 47, 1240-1249.

[25] Sneddon,J. Background Correction Techniques in Atomic Spectroscopy. *Spectroscopy*. **1987**, 2(5), 38-45.

[26] Cassella, R.J.; Brum, D.M.; Lima, C.F.; Fonseca, T.C.D. Direct Determination of Cu and

Fe in Jet Fuel by Electrothermal Atomic Absorption Spectrometry with Injection of Sample as Detergent Emulsions. *Elsevier.* **2011**, 90, 1215-1220.

[27] *Analytical Methods for Flame Spectroscopy*; Copper in Chicken Blood Plasma Flame; Varian Techtron, Australia, **1985.**

[28] Alvarez, M.A.; Carrion,M.; Gutierrez, H. Effects of Atomization Surfaces and Modifiers on the Kinetics of Copper Atomization in Electrothermal Atomic Absorption Spectrometry. *Spectrochimica Acta Part B*. **1996**, 51, 1121-1132.